Scientia Iranica C (2021) 28(3), 1343–1352

Sharif University of Technology
Scientia Iranica
Transactions C: Chemistry and Chemical Engineering
http://scientiairanica.sharif.edu

Theoretical studies on photo-induced electron transfer process on [Thioridazine].C_{60} nano-complex; a first principle DFT and TD-DFT

A.A. Taherpour[a,b,*], P. Gholami Keivanani[a], M. Jamshidi[c], S. Hatami[a], and N. Zolfaghar[a]

a. *Faculty of Chemistry, Razi University, Kermanshah, P.O. Box 6714967346, Iran.*
b. *Medical Biology Research Center, Kermanshah University of Medical Sciences, Kermanshah, Iran.*
c. *Young Researchers and Elite Club, Kermanshah Branch, Islamic Azad University, Kermanshah, Iran.*

Received 18 April 2019; received in revised form 12 November 2019; accepted 26 October 2020

KEYWORDS
Photo-induced electron transfer;
Thioridazine;
DFT;
Marcus theory.

Abstract. In this study, using Density Functional Theory (DFT) and Time Dependent Density Functional Theory (TD-DFT) methods, the physical and chemical properties of a Thioridazineand fullerene C_{60} nano complex were studied. The most important goal was to increase C_{60} dipolar moment as a novel drug delivery system to carry Thioridazineand. Several descriptors were used in the ground state, including electrochemical properties based on HOMO and LUMO orbital energy, hardness, softness, chemical potential, and Mulliken charge. The dipole moment of this nano-complex is about 2.61D, which indicates its moderate solubility in polar solvents. The UV-Vis spectrum obtained with the CAM-B3LYP method shows that the absorption spectrum has blue-shifted by about $\lambda = 24$ nm after formation of the complex. Based on the calculations in the excited state and the hole-electron theory in the first three modes, a Photo-induced Electron Transfer (PET) phenomenon was observed at different absorption wavelengths for the complex. Using the Marcus theory of electron transfer, the free energy of activation for electron transfer and the free energy of electron transfer for all PETs were calculated.

1. Introduction

In recent years, targeted drug delivery has been growing at an ever-increasing pace and, almost daily, new systems of drug release are being introduced [1]. The goal of nanotechnology in medicine is to provide pathological facilities and treat diseases on a fundamental scale, i.e. molecular or even micro-molecular. In the field of pharmacy, nanotechnology has very essential applications, and the strategic goal in this area is the patient-centered and disease-centered design of smart and targeted drugs [2,3]. These drugs have a marked mode of action and have the ability to sense the damaged environment in the tissue, decide on how to transfer themselves and the amount required (dose), and prevent side effects and sensitization [4]. These drugs are able to detect the required amount before they release themselves in the tissue and will not activate themselves if they do not meet the requirements for their release. The characteristics of such drugs

*. *Corresponding author. Tel./Fax: +98(83)34274559*
E-mail address: avat.taherpour@gmail.com (A.A. Taherpour)

doi: 10.24200/sci.2020.53361.3203

are the precise prediction of their function, a feature which is not available in current non-smart drugs [5]. In recent years, much attention has been paid to the provision of nanostructures as carriers for drug delivery. These structures can be considered as highly effective drug delivery systems since they can control and slow down the release of a drug, protect drug molecules, have a smaller particle size than a cell, cross biological barriers for delivering drugs to the target site, as well as long time circulation in the bloodstream, targeted drug delivery and biocompatibility, which all increase the efficacy of the drug [6–8]. Side effects of medication on other organs, tissue and cells of the body is one of the most important reasons for this volume of research on targeted drug delivery. In addition, reducing drug intake is another purpose of using this medication method; in other words, increasing the efficacy of the drug reduces its intake [9]. For example, about 98% of common antibiotics are excreted through the kidneys, which is the main cause of bacterial resistance [10–12].

The use of nanotechnology in the design of new drug release systems is very promising [13]. Since the discovery of nanostructures such as nanotubes, fullerenes, graphene etc., scientists have focused on the issue of drug release [8,14,15]. Functionalized carbon nanotubes have been used frequently as carriers of drugs and genes into the body and cells of living organisms [16,17]. Also, functionalized fullerenes with hydrophilic groups soluble in polar solvents are one of the most successful drug delivery systems of its kind [18,19]. Some fullerenes, such as C_{60}, have high antibacterial and antiviral properties and have recently been used as a therapeutic method for inhibiting and destroying cancerous tumors [20–23]. It is also easily recognizable in various environments due to its own optical properties [24,25].

Because of their small size, these particles can easily pass through membranes and biological barriers and reach the cell interior. These structures, with a high active surface, can provide surface engineering for drug delivery. The surface of these nanoparticles is functionalized with various groups and compounds for increasing solubility and biocompatibility as well as carrying different materials. These nanoparticles can be used as carriers to carry biological molecules such as proteins, DNA, biological agents and drugs. Pharmaceutical compounds are loaded onto or within these structures. Targeting and simultaneously transferring two or more compounds is one of the other characteristics of these particles in drug delivery. Recently, the complexation of some drugs with fullerenes without substitution is one of the methods proposed for the transfer of drugs to some membranes, such as walls of bacteria and the brain membrane. Hosseinian et al. used fullerene C_{24} as a new carrier for the 5-fluorouracil drug [26]. Using the Density Functional Theory (DFT) and Time Dependent Density Functional Theory (TD-DFT) computational methods, Samanta and Das investigated the optical and structural properties of the temozolomide, procarbazine, carmustine, and lomustine complex and introduced it as an effective way of delivering these drugs to the brain membrane [27]. Gong et al. demonstrated an efficient and novel fluorinated graphene oxide-based nanocarrier with nanosized structure, modifiable surface, high PL emission, high drug loading capacity and NIR absorption, and detailed DFT investigations on the interactions of FGO with single or mixed drugs [28]. In addition, Teixeira et al. investigated involving the adsorption of anastrozole on gold surfaces as nanocarriers of anastrozole. They simulated the molecular interactions with gold atoms in two possible ways using DFT calculations. They also claimed experimental results on triazole or nitrile moieties, which were supported by DFT calculations to assign main vibrational modes. The obtained results also indicated that the nitrile groups are the most preferred anchorage moieties for the discussed adsorption [29]. Taherpour et al. examined some of the optical properties, including UV-Vis adsorption, fluorescence emission, and the Photo-induced Electron Transfer (PET) phenomenon for the [C_{60}+Cefamandole] complex using DFT and TDDFT calculations [30].

In the PET and PCT processes, an electron or a charge transfers from donor to acceptor groups in the presence of UV-Vis irradiation [31,32]. This process is important in many ways. PET and PCT processes directly affect the quality of fluorescence and phosphorescence emission spectra, and when it occurs from chelator to fluorophore, it causes the quenching of the fluorescence emission spectrum [33–35]. It is well suited for drug delivery systems with the ability of optical detection of drug and carrier in various environments. In addition, the study of electron transfer processes, such as the electron transfer wavelength, and the energy required to perform this process in biological systems is of particular importance [36,37]. With the help of the Marcus theory and the Rehm-Weller equation for complexes, one can study some of these kinetic and thermodynamic parameters [38].

In this study, the electronic, structural and optical properties of Thioridazine, C_{60} and the [Thioridazine+C_{60}] complex have been investigated using DFT and TD-DFT computational methods. Thioridazine is a piperidine typical antipsychotic drug belonging to the phenothiazine drug group and was previously widely used in the treatment of schizophrenia and psychosis, and also to stop alcohol and drug abuse [39]. The geometric optimizer of the [Thioridazine+C_{60}] complex provides accurate information, such as electron density and bipolar moment. In addition to the UV-Vis absorption spectrum, some of the optical

properties, including the PET process [40], were investigated using the electron-hole theory, and the free energy of activation for electron transfer was calculated using the Marcus theory.

2. Computational details

In the present study, the structures of fullerene C_{60}, Thioridazineand the [Thioridazine+C_{60}] complex were studied using the DFT method [41].

The optimization of the structures was done using the B3LYP method in the gas phase and also the 6-31++G^{**} basis set was used, this diffuse Pople basis function was applied because of considering partial positive charge spread on the surface of the fullerene. In an excited state, the computational cost increases significantly, especially for the PET calculation. The same method has been used to obtain reliable data for comparisons and reports [42–45]. The purpose of this study is to evaluate the capabilities of the fullerene C_{60} as a new system for the delivery of Thioridazine, and the unprotonated form was chosen to investigate the effect of the ET process between the donor and acceptor species. The protonated form was not suitable for the aims of this study and has a high dipole moment before the ET process. The protonated form of the Thioridazine has plus charge(s) and it creates a condition to invert the direction of the ET process between these two species. DFT calculations at this level provide a good view of the features of this complex [46]. One important parameter evaluated in the ground state is the polarity of the nano-composite and also the energy of complex formation (EF). For further investigation, the Electron Localization Function (ELF) was plotted. This parameter perfectly shows the electronic changes at the points where interaction occurs between the two components of the complex [47,48].

The density of energy states for all components was obtained using the method of Charge Decomposition Analysis (CDA), and the splitting of the ligand field for the [Thioridazine+C_{60}] complex was studied [49]. These calculations, in addition to providing HOMO or LUMO orbital energy for all components, indicate the sharing of levels in the formation of the complex with an appropriate approximation [50]. NBO analysis is one of the most important parameters for the investigation of the electron properties of two-component species, such as complexes or molecules with two electron-acceptor components [51,52]. Some electron transitions of fullerene were determined before and after the formation of the complex using this type of calculation. In addition, electron transitions from fullerene to Thioridazine and from Thioridazine to fullerene were identified in the [Thioridazine+C_{60}] complex. Calculations in the excited state for the donor-acceptor species are of particular importance. At this level of calculation, phenomena such as electron transition from the HOMO to LUMO levels, as well as charge and electron transfers, are observed. The computational method and CAM-B3LYP/6-31G* basis set were used for these calculations, although, using the 6-31++G^{**} basis set distinguished much higher accuracy than that of 6-31G*. In an excited state, the computational cost increases significantly, especially for the PET calculation. The same method was used to have reliable data for comparisons and reports. The CAM-B3LYP method has an excellent accuracy in electron transitions in the excited state and is widely used in organic compounds [53]. Optical absorption spectra for Thioridazine, fullerene C_{60}, and [Thioridazine+C_{60}] complex were obtained in the gas phase and under environmental conditions. The PET process was investigated using the electron-hole theory with the same method. Charge transfer from chelator to fullerene was obtained for different modes. Using the Marcus theory of electron transfer, the free energy of activation and the Gibbs free energy were calculated for each electron transfer [54].

3. Results and discussions

The optimized C_{60} molecule has a dipole moment of zero ($\mu = 0$). After the formation of the [Thioridazine+C_{60}] complex, the dipole moment increased by 2.61 D. The main idea is for the ET complex between C_{60} and Thioridazine medicine to be solved in biologic media and water content solvents. The formation energy of this complex was calculated to be about 5.19 kcal mol^{-1}, indicating a weak linkage of the Landon type. Therefore, this system could easily create removal from the fullerene after the transfer of the drug and the drug is delivered to the intended destination (Figure 1). Also, according to recent findings,

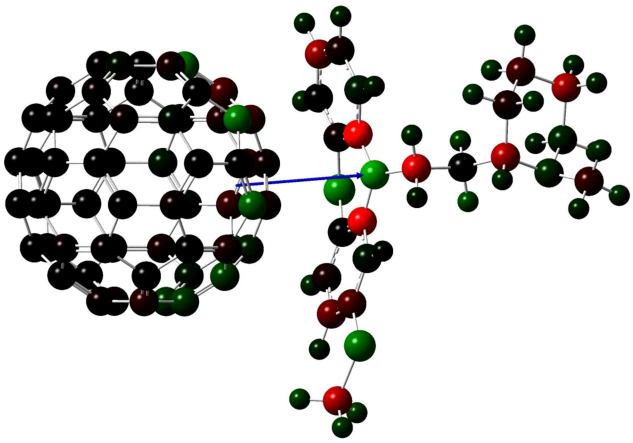

Figure 1. Dipole moment and Mulliken charge of the [Thioridazine+C_{60}] complex in gaseous phase calculated by B3LYP/6-31++G (d, p) method.

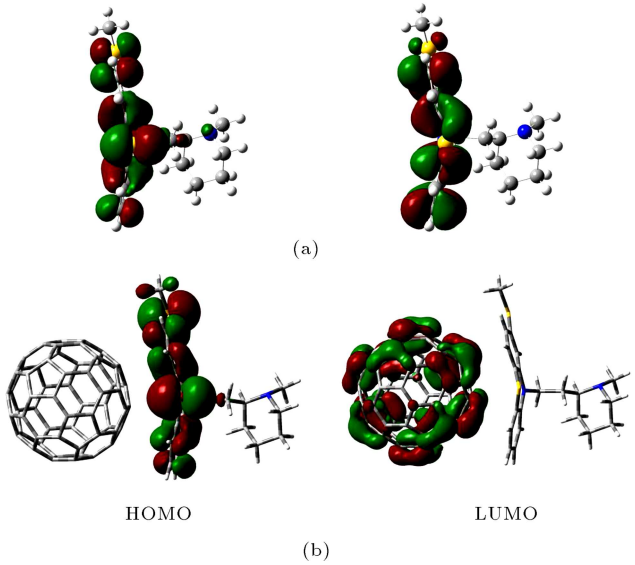

Figure 2. (a) HOMO and LUMO orbitals of Thioridazine. (b) [Thioridazine+C_{60}].

fullerene will deform after the charge transfer and C_{60}^{-1} formation, which will ultimately lead to changes in the IR vibrational spectrum, in addition to the changes in charge density and other properties of fullerene.

Figure 2(a) shows the HOMO and LUMO orbitals of Thioridazine that are both on the aromatic part of the Thioridazine drug.

In Figure 2(b), which is related to the [Thioridazine+C_{60}] complex, the HOMO orbital is localized on Thioridazine, but the LUMO orbital is localized on the fullerene C_{60}, which represents the charge transitions from drug to fullerene, which will be dealt with in detail in the NBO analysis.

In the CDA method, the splitting of the ligand field for complexes can be calculated with a relatively fair approximation. In Figure 3(a), the orbital contribution of Thioridazine and fullerene C_{60} is shown with an approximation in the formation of the [Thioridazine+C_{60}] complex. The matching of the DOS diagram can be seen in Figure 3(b). Accordingly, the energy of HOMO and LUMO orbitals and the band gaps of all three molecules are presented in Table 1. Also, hardness (η), softness (S), electrophilicity (ω) and chemical potential (μ) were calculated.

These amounts of energy contribute to the formation of the complex and also predict the activity and performance of this nano-complex, which can be referred to drug targeting based on the hardness and softness of the intended site. The target and the intended location can be determined based on hardness and softness, as well as electronegativity, of the two components (drug and drug release site).

Comparison of ELF electron density images for one of the six-membered rings of C_{60} before and after the formation of the complex well illustrates the change in the fullerene electron system. Figure 4(a) refers to the C_{60} alone, which has changed greatly after the formation of the complex in Figure 4(b), and has undergone a change in the electron current of the ring system and thus of the whole fullerene. These images intuitively help to understand charge transfers in the NBO analysis. Table 2 shows the charge transfers from Thioridazine to C_{60} as well as internal charge transitions for the C_{60} before and after the formation of the complex. As we can see, various transitions involving the nonbonding electron pairs of N and S atoms, σ and π bonds from Thioridazine to Fullerene C_{60} in the [Thioridazine+C_{60}] complex have occurred. These transitions cause many changes in the ring current and electron density of the C_{60} before and after the formation of the complex, as was pointed out in the

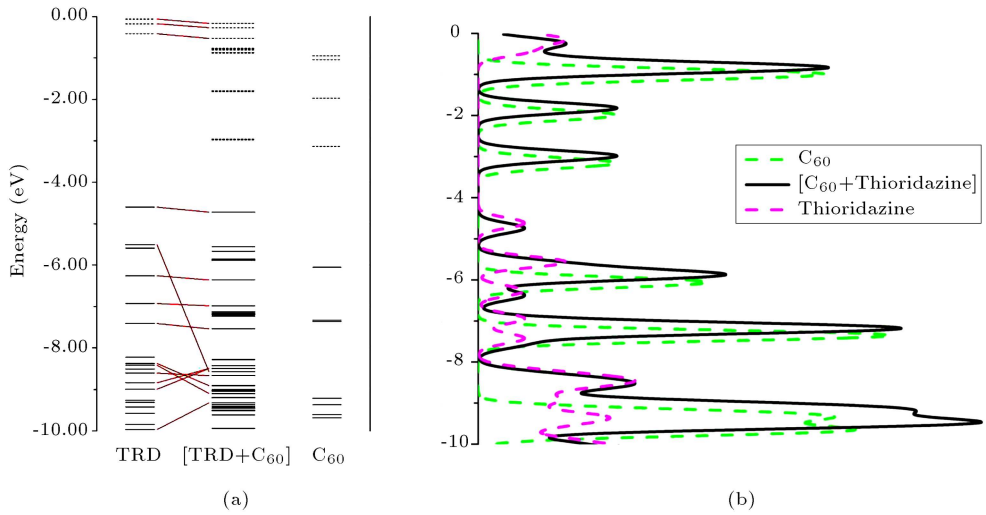

Figure 3. (a) Charge Decomposition Analyses (CDA). (b) Density Of State (DOS) for Thioridazine, C_{60} and [C_{60}+Thioridazine] in the range of –10 to 0 eV.

Table 1. Hardness (η), softness (S) and electro-physical (ω), chemical potential (μ), HOMO or LUMO orbitals energy, energy gap and bipolar moments for C_{60}, [C_{60}+Thioridazine] and Thioridazine.

Data	E_{HOMO}	E_{LUMO}	ΔE	Dipole moment	μ	η	ω	S
C_{60}	–6.05	–3.14	–2.91	0	4.59	1.45	7.26	0.34
C_{60}+Thioridazine	-7.68	–2.74	–4.94	6.36	5.21	2.47	5.49	0.4
Thioridazine	–7.51	–0.17	–7.34	3.75	2.61	2.32	1.47	0.43

Table 2. NBO calculated donor and acceptor orbital energies for C_{60} and [C_{60}+Thioridazine] complex with kcal.mol^{-1} unit.

Drug→C_{60}		C_{60} → C_{60}	Before	After
$\pi_{drug} \rightarrow \pi^*_{C_{96}-C_{99}}$	0.18	$\sigma_{C_{93}-C_{96}} \rightarrow \sigma^*_{C_{79}-C_{92}}$	2.76	1.21
$\pi_{drug} \rightarrow \pi^*_{C_{80}-C_{86}}$	0.11	$\sigma_{C_{86}-C_{89}} \rightarrow \sigma^*_{C_{79}-C_{92}}$	2.78	1.22
$\pi_{drug} \rightarrow \pi^*_{C_{89}-C_{106}}$	0.09	$\sigma_{C_{89}-C_{92}} \rightarrow \sigma^*_{C_{79}-C_{81}}$	3.23	1.11
$\pi_{drug} \rightarrow \pi^*_{C_{83}-C_{93}}$	0.83	$\pi_{C_{83}-C_{93}} \rightarrow \pi^*_{C_{79}-C_{92}}$	13.74	0.31
$\pi_{drug} \rightarrow \pi^*_{C_{79}-C_{92}}$	0.11	$\pi_{C_{81}-C_{82}} \rightarrow \pi^*_{C_{79}-C_{92}}$	13.62	0.31
$\pi_{drug} \rightarrow \pi^*_{C_{81}-C_{82}}$	0.14	$\sigma_{C_{81}-C_{82}} \rightarrow \sigma^*_{C_{82}-C_{83}}$	2.62	1.18
$\pi_{drug} \rightarrow \pi^*_{C_{83}-C_{93}}$	0.30	$\sigma_{C_{83}-C_{93}} \rightarrow \sigma^*_{C_{86}-C_{96}}$	1.25	1.18
$LP(\sigma)N \rightarrow \pi^*_{C_{79}-C_{92}}$	0.14	$\sigma_{C_{81}-C_{82}} \rightarrow \sigma^*_{C_{79}-C_{81}}$	2.61	1.18
$LP(\pi)S \rightarrow \pi^*_{C_{83}-C_{93}}$	0.06	$\sigma_{C_{83}-C_{93}} \rightarrow \sigma^*_{C_{92}-C_{93}}$	2.64	1.18
$\pi_{drug} \rightarrow \pi^*_{C_{79}-C_{92}}$	1.18	$\pi_{C_{81}-C_{82}} \rightarrow \sigma^*_{C_{79}-C_{81}}$	1.41	0.73
$\pi_{drug} \rightarrow \pi^*_{C_{83}-C_{93}}$	0.11	$\sigma_{C_{83}-C_{93}} \rightarrow \sigma^*_{C_{93}-C_{96}}$	2.62	1.18
$\pi_{drug} \rightarrow \pi^*_{C_{79-92}}$	0.84	$\sigma_{C_{82}-C_{83}} \rightarrow \sigma^*_{C_{83}-C_{93}}$	2.9	1.21
$\pi_{drug} \rightarrow \pi^*_{C_{81}-C_{82}}$	0.83	$\pi_{C_{81}-C_{82}} \rightarrow \sigma^*_{C_{82}-C_{83}}$	1.4	0.73
$\pi_{drug} \rightarrow \pi^*_{C_{83}-C_{93}}$	0.20	$\sigma_{C_{83}-C_{93}} \rightarrow \sigma^*_{C_{89}-C_{92}}$	1.26	1.18
$\pi_{drug} \rightarrow \pi^*_{C_{81}-C_{82}}$	0.68	$\pi_{C_{81}-C_{82}} \rightarrow \pi^*_{C_{83}-C_{93}}$	13.76	0.31
$\pi_{drug} \rightarrow \pi^*_{C_{83}-C_{93}}$	0.05	$\sigma_{C_{83}-C_{93}} \rightarrow \sigma^*_{C_{82}-C_{83}}$	2.62	1.18
$\pi_{drug} \rightarrow \pi^*_{C_{95}-C_{101}}$	0.07	$\sigma_{C_{93}-C_{96}} \rightarrow \sigma^*_{C_{86}-C_{96}}$	1.19	1.11
$\pi_{drug} \rightarrow \pi^*_{C_{79}-C_{92}}$	0.07	$\sigma_{C_{89}-C_{92}} \rightarrow \sigma^*_{C_{79}-C_{92}}$	2.84	1.22
$\pi_{drug} \rightarrow \pi^*_{C_{81}-C_{82}}$	2.43	$\sigma_{C_{82}-C_{83}} \rightarrow \sigma^*_{C_{81}-C_{82}}$	2.9	1.21

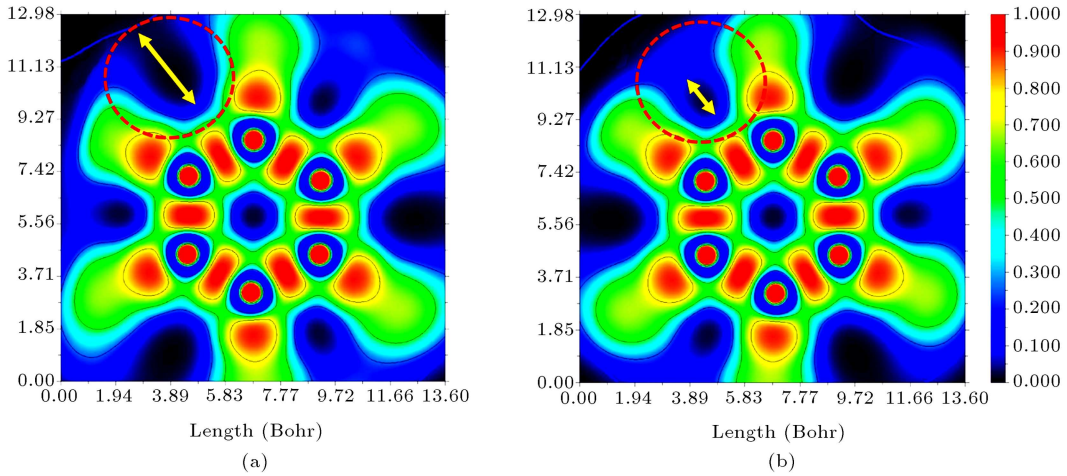

Figure 4. Electron density images: (a) ELF for one of the six-membered rings of C_{60} and (b) the same six-membered C_{60} ring in the [Thioridazine+C_{60}] complex.

comparison of ELF electron density. For example, the transition of $\pi C_{83} - C_{93} \rightarrow \pi^* C_{79} - C_{92}$ has reached 13.74 kcal.mol^{-1} to 0.31 kcal.mol^{-1}.

The transitions reported in the NBO analysis are the result of an orbital overlapping of the two components of the [Thioridazine+C_{60}] complex, as shown in Figure 5. This image depicts the area of overlap and load exchange between the drug and fullerene, which is very effective in understanding the electron properties of such systems. The formation energy of a complex that has the London force is noticeable in this image.

In Figure 6, images of the UV-Vis absorption spectrum for Thioridazine, fullerene C_{60} and the [Thioridazine+C_{60}] complex were presented. As seen, Thioridazine absorbs the UV-Vis spectrum at wavelengths lower than the fullerene and [Thioridazine+C_{60}] complex. With respect to the molecular levels of the components forming the complex [Thioridazine+C_{60}] in Figure 3 and Table 1, it is found that because of the increasing in the band gap, the absorbing requires more energy to elevate to the excited states. This also occurs for fullerene C_{60} and the [Thioridazine+C_{60}] complex. The complex [Thioridazine+C_{60}] has a blue-shift of about 0.142 eV (24 nm) compared to the fullerene. In addition, the appearance of a small peak at 2.793 eV (444 nm) for the [Thioridazine+C_{60}]complex is observed, which is the result of the addition of several molecular levels resulting from the splitting of the ligand field in the energy of about –6.5 eV in Figure 3.

The electron-hole theory calculates the contribution of hole or electron orbitals with a good approximation. In Figure 7, hole and electron orbitals are shown for the first three excited states. As the images show, these orbitals are separated from each other with a high percentage, indicating the occurrence of the PET phenomenon between the two components of the complex. PET and PCT are highly effective in identifying and tracking drugs and other biological components [55]. These phenomena generally quench the fluorescence emission spectrum. Moreover, the study of the excited state for biological systems such as drug release systems can open new windows for activating the drug in different parts of the body of

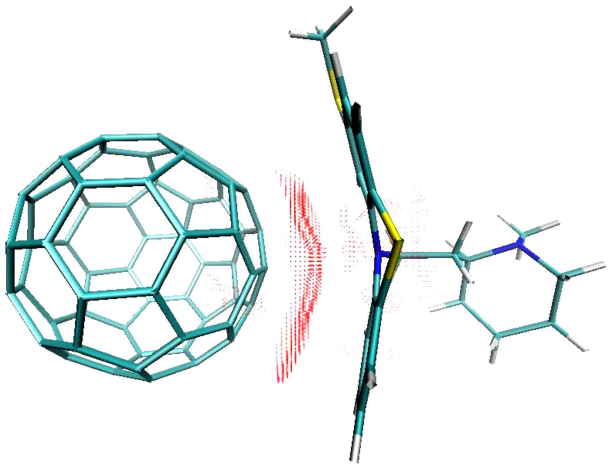

Figure 5. Orbital overlapping between Thioridazine and C_{60} in the [Thioridazine+C_{60}] complex.

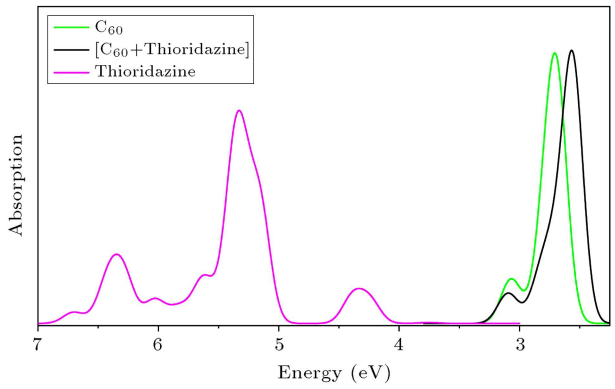

Figure 6. UV-Vis absorption spectrum for fullerene C_{60} and [Thioridazine+C_{60}] complex.

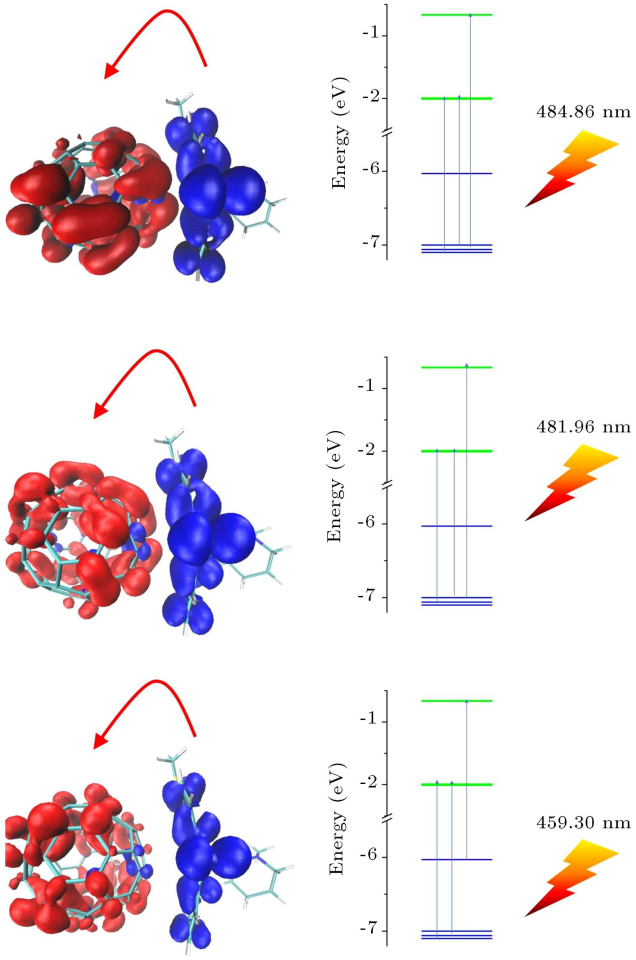

Figure 7. Electron-hole orbitals and PET process for n-state=1, 2, 3.

Table 3. The data values on the electron transfer (ΔG^0) and kinetic of electron transfer (k_{et}) in [Thioridazine+C_{60}] complex.

n-state	Wavelength (nm)	k_{et} (sec^{-1})	$\Delta G^{\#}$ (kcal mol^{-1})	ΔG^0 (kcal.mol^{-1})
1	484.86	3.4869×10^{-31}	58.9284	45.7070
2	481.96	1.9328×10^{-31}	59.2830	45.849
3	459.30	1.3718×10^{-33}	62.2078	47.012

living organisms. This complex transfers electrons from the drug to fullerene by absorbing 484.86, 481.96 and 459.30 nm wavelengths, separately.

Given the wavelengths for electron transfer and using Eqs. (1)–(3), one can calculate parameters such as the free energy of activation for electron transfer, electron transfer rate, and energy of electron transfer with good approximation. The value of the electron transfer rate, constant k_{et} is controlled by the activation free energy $\Delta G^{\#}_{et}$, which is a function of the reorganization energy ($l/4$) and electron transfer driving force ΔG_{et} [56]. These results, which are calculated on the basis of the Marcus theory, are presented in Table 3.

$$\Delta G^{\#}_{et} = \Delta E = hc/\lambda, \tag{1}$$

$$k_{et} = k_0 \exp\left(-\Delta G^{\#}_{et}/R\right), \tag{2}$$

$$\Delta G^{\#}_{et} = (1/4)(1 + \Delta G_{et}/l)^2. \tag{3}$$

As can be seen from the results of Table 3, the absorption wavelength has an inverse relationship with the electron transfer rate. This indicates that less energy is spent on this phenomenon, the less free energy of activation will pass through the barrier, and it will occur more quickly. A remarkable point for the studied system is that the phenomenon can be observed in the first three excited states, i.e. the first absorbing wavelengths.

4. Conclusion

The results of the DFT and TD-DFT simulations show that fullerene C_{60} can be used as a novel drug carrier for releasing Thioridazine after the formation of a drug delivery complex. The nano-complex has formation energy of about 5.19 kcal.mol^{-1}, so it can be estimated that after the drug is delivered to the target, it will separate from the fullerene with a small amount of energy. On the other hand, the complex has a dipole moment of about 2.61 D, which indicates a slight solubility in polar solvents such as water. The HOMO orbital of the complex is localized on the drug and the LUMO orbital is localized on the C_{60}. The results of the NBO analysis indicate that the most electron transitions occurred from Thioridazine to fullerene C_{60}. These transitions caused wide changes in the electron current direction of the π system of the fullerene, which is quite evident when comparing the ELF electron density for fullerene C_{60}, before and after the formation of the complex. In the excited state, the UV-Vis absorption wavelength has a slight blue-shift relative to fullerene, which can be due to the narrowing of the band gap. In the first three excited states, the electron transfers from drug to fullerene and also the PET phenomenon occurs. Using the Marcus theory, as well as the required wavelength to carry out these electron transitions in the excited state, the electron transfer rate, the free energy of activation for electron transfer, and the free energy required for this electron transfer were calculated and reported.

Acknowledgment

The authors would like to acknowledge the Theoretical and Computational Research Center of the Chemistry Faculty of Razi University, Kermanshah, Iran, and the Medical Biology Research Center, Kermanshah University of Medical Sciences, Kermanshah, Iran.

References

1. Chien, Y., *Novel Drug Delivery Systems*, Informa Health Care, (1991).
2. Freeman, A.I. and Mayhew, E. "Targeted drug delivery", *Cancer*, **58**, pp. 573–583 (1986).
3. Mills, J.K. and Needham, D. "Targeted drug delivery", *Expert Opinion on Therapeutic Patents*, **9**, pp. 1499–1513 (1999).
4. Allen, T.M. and Cullis, P.R. "Drug delivery systems: entering the mainstream", *Science*, **303**, pp. 1818–1822 (2004).
5. Singh, R. and Lillard, J.W. "Nanoparticle-based targeted drug delivery", *Exp. Mol. Pathol*, **86**, pp. 215–223 (2009).
6. Sun, X., Liu, Z., Welsher, K., et al. "Nano-graphene oxide for cellular imaging and drug delivery", *Nano Research*, **1**, pp. 203–212 (2008).
7. Mishra, B., Patel, B.B., and Tiwari, S. "Colloidal nanocarriers: a review on formulation technology, types and applications toward targeted drug delivery", *Nanomed. Nanotechnol. Biol. Med.*, **6**, pp. 9–24 (2010).

8. Koo, O.M., Rubinstein, I., and Onyuksel, H. "Role of nanotechnology in targeted drug delivery and imaging: a concise review", *Nanomed. Nanotechnol. Biol. Med*, **1**, pp. 193–212 (2005).
9. Nasongkla, N., Bey, E., Ren, J., et al. "Multifunctional polymeric micelles as cancer-targeted, MRI-ultrasensitive drug delivery systems", *Nano Letters*, **6**, pp. 2427–2430 (2006).
10. Kropp, H., Sundelof, J.G., Hajdu, R., and Kahan, F.M. "Metabolism of thienamycin and related carbapenem antibiotics by the renal dipeptidase", *Dehydropeptidase-I, Antimicrobial Agents and Chemotherapy*, **22**, pp. 62–70 (1982).
11. Price-Whelan, A., Dietrich, L.E., and Newman, D.K. "Rethinking' secondary' metabolism: physiological roles for phenazine antibiotics", *Nat. Chem. Biol*, **2**, p. 71 (2006).
12. Jurima-Romet, M., Crawford, K., Cyr, T., et al. "Terfenadine metabolism in human liver. In vitro inhibition by macrolide antibiotics and azole antifungals", *Drug Metab. Disposition*, **22**, pp. 849–857 (1994).
13. Farokhzad, O.C. and Langer, R. "Impact of nanotechnology on drug delivery", *Acs Nano*, **3**, pp. 16–20 (2009).
14. Shi, J., Votruba, A.R., Farokhzad, O.C., and Langer, R. "Nanotechnology in drug delivery and tissue engineering: from discovery to applications", *Nano Letters*, **10**, pp. 3223–3230 (2010).
15. Taherpour, A.A., Zolfaghar, N., Jamshidi, M., Jalilian, J., et al. "Structural distortions of fullerene C60n (n = 0 to –6) by first principle density functional theory", *Journal of Molecular Structure*, **1184**, pp. 546–556 (2019).
16. Bianco, A., Kostarelos, K., and Prato, M. "Applications of carbon nanotubes in drug delivery", *Curr. Opin. Chem., Biol.*, **9**, pp. 674–679 (2005).
17. Liu, Z., Chen, K., Davis, C., et al. "Drug delivery with carbon nanotubes for in vivo cancer treatment", *Cancer Res.*, **68**, pp. 6652–6660 (2008).
18. Hughes, G.A. "Nanostructure-mediated drug delivery", *Nanomed. Nanotechnol. Biol. Med.*, **1**, pp. 22–30 (2005).
19. Cataldo, F. and Da Ros, T., *Medicinal Chemistry and Pharmacological Potential of Fullerenes and Carbon Nanotubes*, Springer Science & Business Media (2008).
20. Bakry, R., Vallant, R.M., Najam-ul-Haq, M., et al. "Medicinal applications of fullerenes", *International Journal of Nanomedicine*, **2**, p. 639 (2007).
21. Harhaji, L., Isakovic, A., Raicevic, N., et al. "Multiple mechanisms underlying the anticancer action of nanocrystalline fullerene", *Eur. J. Pharmacol*, **568**, pp. 89–98 (2007).
22. Brunet, L.N., Lyon, D.Y., Hotze, E.M., et al. "Comparative photoactivity and antibacterial properties of C60 fullerenes and titanium dioxide nanoparticles", *Environmental Science & Technology*, **43**, pp. 4355–4360 (2009).
23. Lyon, D.Y., Adams, L.K., Falkner, J.C., et al. "Antibacterial activity of fullerene water suspensions: effects of preparation method and particle size", *Environmental Science & Technology*, **40**, pp. 4360–4366 (2006).
24. Erb, T., Zhokhavets, U., Gobsch, U., et al. "Correlation between structural and optical properties of composite polymer/fullerene films for organic solar cells", *Adv. Funct. Mater.*, **15**, pp. 1193–1196 (2005).
25. Scharber, M., Schultz, N., Sariciftci, N., et al. "Optical- and photocurrent-detected magnetic resonance studies on conjugated polymer/fullerene composites", *Physical Review B*, **67**, p. 085202 (2003).
26. Hosseinian, A., Vessally, E., Yahyaei, S., et al. "A density functional theory study on the interaction between 5-fluorouracil drug and C24 fullerene", *J. Clust. Sci.*, **28**, pp. 2681–2692 (2017).
27. Samanta, P.N., and Das, N.N. "Noncovalent interaction assisted fullerene for the transportation of some brain anticancer drugs: A theoretical study", *Journal of Molecular Graphics and Modelling*, **72**, pp. 187–200 (2017).
28. Gong, P., Zhang, L., Yuan, X.A., et al. "Multifunctional fluorescent PEGylated fluorinated graphene for targeted drug delivery: An experiment and DFT study", *Dyes and Pigments*, **162**, pp. 573–582 (2019).
29. Teixeira, T.A.R., Costa, L.A.S., and Sant'Ana, A.C. "A proposal for the adsorption of anastrozole anticancer drug on gold nanoparticle surfaces", *Journal of Raman Spectroscopy*, **50**(10), pp. 1462–1467 (2019).
30. Taherpour, A.A., Jamshidi, M., and Rezaei, O. "DFT and TD-DFT theoretical studies on photo-induced electron transfer process on [Cefamandole]. C_{60} nanocomplex", *Journal of Molecular Graphics and Modelling*, **75**, pp. 42–48 (2017).
31. Wazzan, N. and Safi, Z. "DFT calculations of the tautomerization and NLO properties of 5-amino-7-(pyrrolidin-1-yl)-2,4,4-trimethyl-1,4-dihydro-1,6-naphthyridine-8-carbonitrile (APNC)", *Journal of Molecular Structure*, **1143**, pp. 397–404 (2017).
32. Jamshidi, M., Rezaei, O., Belverdi, A.R., et al. "A highly selective fluorescent chemosensor for Mg 2+ ion in aqueous solution using density function theory calculations", *Journal of Molecular Structure*, **1123**, pp. 111–115 (2016).
33. An, B., Yuan, H., Zhu, Q., et al. "Theoretical insight into the excited-state intramolecular proton transfer mechanisms of three amino-type hydrogen-bonding molecules", *Spectrochimica Acta Part A: Molecular and Biomolecular Spectroscopy*, **175**, pp. 36–42 (2017).
34. Yuan, H., Feng, S., Wen, K., et al. "A quantum-chemical insight into the tunable fluorescence color and distinct photoisomerization mechanisms between a novel ESIPT fluorophore and its protonated form", *Spectrochimica Acta Part A: Molecular and Biomolecular Spectroscopy*, **183**, pp. 123–130 (2017).

35. Taherpour, A.A., Jamshidi, M., and Rezaei, O. "Recognition of switching on or off fluorescence emission spectrum on the Schiff-bases as a Mg2+ chemosensor: A first principle DFT and TD-DFT study", *Journal of Molecular Structure*, **1147**, pp. 815–820 (2017).
36. Harriman, A., Kubo, Y., and Sessler, J.L. "Molecular recognition via base pairing: photoinduced electron transfer in hydrogen-bonded zinc porphyrin-benzoquinone conjugates", *Journal of the American Chemical Society*, **114**, pp. 388–390 (1992).
37. Reisner, E., Arion, V.B., Keppler, B.K., et al. "Electron-transfer activated metal-based anticancer drugs", *Inorg. Chim. Acta*, **361**, pp. 1569–1583 (2008).
38. Taherpour, A.A. "Theoretical and quantitative structural relationship study of the electrochemical properties of [M2@ C x]@[SWCNT (5, 5)-Armchair-C n H20] (M=Er and Sc, x = 82 and 84, and n = 20 − 300) complexes", *The Journal of Physical Chemistry C*, **113**, pp. 5402–5408 (2009).
39. Carlsson, A., Roos, B.E., Wålinder, J., et al. "Further studies on the mechanism of antipsychotic action: Potentiation by α-methyltyrosine of thioridazine effects in chronic schizophrenics", *J. Neural Transm*, **34**, pp. 125–132 (1973).
40. Gholivand, K., Hosseini, M., Maghsoud, Y., et al. "Relations between structural and luminescence properties of novel lanthanide nitrate complexes with bis-phosphoramidate ligands, inorganic chemistry", *Inorg. Chem.*, **58**(9), pp. 5630–5645 (2019).
41. Patel, R.N. and Singh, Y.P. "Synthesis, structural characterization, DFT studies and in-vitro antidiabetic activity of new mixed ligand oxovanadium(IV) complex with tridentate Schiff base", *Journal of Molecular Structure*, **1153**, pp. 162–169 (2018).
42. Zara, Z., Iqbal, J., Ayub, K., et al. "A comparative study of DFT calculated and experimental UV/Visible spectra for thirty carboline and carbazole based compounds", *Journal of Molecular Structure*, **1149**, pp. 282–298 (2017).
43. Ahmadi, R. "Study of thermodynamic parameters of (TATB) and its fullerene derivatives with different number of Carbon (C20, C24, C60), in different conditions of temperature, using density functional theory", *International Journal of Nano Dimension*, **8**, pp. 250–256 (2017).
44. Srivastava, A.K., Kumar, A., and Misra, N. "Superalkali@ C60- superhalogen: Structure and nonlinear optical properties of a new class of endofullerene complexes", *Chemical Physics Letters*, **682**, pp. 20–25 (2017).
45. Sutradhar, S. and Patnaik, A. "A new fullerene-C60-nanogold composite for non-enzymatic glucose sensing", *Sensors and Actuators B: Chemical*, **241**, pp. 681–689 (2017).
46. Dhiman, S., Kumar, R., and Dharamvir, K. "DFT study of Cu and Ag clusters inside C_{60}", *Journal of Molecular Structure*, **1100**, pp. 328–337 (2015).
47. Taherpour, A.A., Jamshidi, M., Rezaei, O., et al. "Photoinduced electron transfer process on emission spectrum of N,N′-bis(salicylidene)-1,2- phenylenediamine as a Mg2+ cation chemosensor: A first principle DFT and TDDFT study", *Journal of Molecular Structure*, **1161**, pp. 339–344 (2018).
48. Taherpour, A.A., Shahri, Z., Rezaei, O., et al. "Adsorption, intercalation and sensing of helium on yttrium functionalized open edge boron nitride: A first principle DFT and TDDFT study", *Chemical Physics Letters*, **691**, pp. 231–237 (2018).
49. Wagner, F.R., Bezugly, V., Kohout, M. and Grin, Y. "Charge decomposition analysis of the electron localizability indicator: a bridge between the orbital and direct space representation of the chemical bond", *Chemistry-A European Journal*, **13**, pp. 5724–5741 (2007).
50. Paredes-Gil, K. and Jaque, P. "Initiation stage of alkene metathesis: Insights from natural bond orbital and charge decomposition analyses", *Chemical Physics Letters*, **618**, pp. 174–181 (2015).
51. Rajesh, P., Kandan, P., Sathish, S., et al. "Vibrational spectroscopic, UV-Vis, molecular structure and NBO analysis of Rabeprazole", *Journal of Molecular Structure*, **1137**, pp. 277–291 (2017).
52. Taherpour, A.A., Rezaei, O., Shahri, Z., et al. "First principles studies of electronic and optical properties of helium adsorption on Sc-doped BN monolayer", *Journal of the Iranian Chemical Society*, **12**, pp. 1983–1990 (2015).
53. Srivastava, R., Al-Omary, F.A.M., El-Emam, A.A., et al. "A combined experimental and theoretical DFT (B3LYP, CAM-B3LYP and M06-2X) study on electronic structure, hydrogen bonding, solvent effects and spectral features of methyl 1H-indol-5-carboxylate", *Journal of Molecular Structure*, **1137**, pp. 725–741 (2017).
54. Scheiner, S. and Duan, X. "Applicability of the Marcus equation to proton transfer in symmetric and unsymmetric systems", *Journal of Molecular Structure: THEOCHEM*, **285**, pp. 27–32 (1993).
55. Shamsipur, M., Barati, A., Taherpour, A.A., et al. "Resolving the multiple emission centers in carbon dots: from fluorophore molecular states to aromatic domain states and carbon-core states", *The Journal of Physical Chemistry Letters*, **9**, pp. 4189–4198 (2018).
56. Taherpour, A.A. and Maleki-Noureini, M. "Free energies of electron transfer, electron transfer kinetic theoretical and quantitative structural relationships and electrochemical properties studies of gadolinium nitride cluster fullerenes Gd3N@Cn in [X-UTY][Gd3N@Cn] (n = 80, 82, 84, 86 and 88) supramolecular complexes", *Fullerenes, Nanotubes and Carbon Nanostructures*, **21**, pp. 485–502 (2013).

Biogrphies

Avat Arman Taherpour is academic member and Professor of Organic Chemistry in the Chemistry Fac-

ulty of Razi University, Kermanshah, Iran. He is currently part time invited researcher with the Medical Biology Research Center, Kermanshah University of Medical Sciences, Kermanshah, Iran. Dr. Taherpour carried out his post-doctoral research in Organic Chemistry and Reactive Intermediates and Unusual Molecules Group under the supervision of Professor Curt Wentrup at The University of Queensland, and has extended scientific collaboration with Australian Universities since 2006. He has also been Chairman of the Scientific Council of the "Elites Foundation of Kermanshah Province", Kermanshah, Iran, since 2018.

Parya Gholami Keivanani obtained an MS degree in Nanochemistry under the supervision of Prof. Taherpour at Razi University, Kermanshah, Iran. Her research interest is theoretical and computational nanochemistry.

Morteza Jamshidi obtained an MS degree in Organic Chemistry under the supervision of Prof. Taherpour at the Islamic Azad University, Arak, Iran. He is collaborating with the Young Researchers and Elite Club in the Kermanshah Branch of the Islamic Azad University, Kermanshah, Iran.

Samira Hatami obtained an MS degree in Nanochemistry under the supervision of Prof. Taherpour at Razi University, Kermanshah, Iran. Her research interest is theoretical and computational nanochemistry.

Narges Zolfaghar obtained her PhD degree in Physical Chemistry. She completed her postdoctoral research under the supervision of Prof. Taherpour at the Chemistry Faculty of Razi University, Kermanshah, Iran, with the support of the Iran National Science Foundation.